Article:
Lawes, M, Sharpe, GJ, Tripathi, N et al. (1 more author) (2016) Influence of spark ignition in the determination of Markstein lengths using spherically expanding flames. Fuel, 186. pp. 579-586. ISSN 0016-2361

https://doi.org/10.1016/j.fuel.2016.08.013

Supplementary Material

M. Lawes[a], G.J. Sharpe[a], N. Tripathi[a,+], R.F. Cracknell[b,*]

[a] School of Mechanical Engineering, University of Leeds, Leeds, LS2 9JT, UK

[b] Shell Global Solutions, Brabazon House, Threapwood Road, Concord Business Park, Manchester, M22 0RR

[*] Corresponding author : Roger Cracknell

E-mail address :Roger.Cracknell@shell.com

Postal address : Shell Global Solutions, Brabazon House, Threapwood Road, Concord Business Park, Manchester, M22 0RR

Phone number : +161 499 4572

E-mail addresses of other authors

M. Lawes : M.Lawes@leeds.ac.uk

G.J. Sharpe : G.J.Sharpe@leeds.ac.uk

N Tripathi : Navanshu.Tripathi@shell.com

+ Now at Shell Global Solutions, Brabazon House, Threapwood Road, Concord Business Park, Manchester, M22 0RR

Type of article : full-length

Shown in Fig. S1(a) is the variation of flame speed against time for a mixture of methane and air at an ignition energy of 36 mJ and an equivalence ratio, ϕ, of 1.1. Data from three explosions are shown at nominally identical conditions by the different symbols. Also shown by the solid curve is the average-speed from the three sets of data. Shown in Fig. S1(b) is the same data plotted against flame radius. Data for flames larger than 40 mm are not shown because they are influenced by the confining effects of the vessel geometry as discussed in [35]. There is good repeatability between the three sets of data in Fig. S1 and the averaged

curve is a reasonable representation of them. It is seen in Fig. S1 that immediately after ignition, S_n initially is very high due to the overdriving effect of the spark [3]. However, S_n decelerates rapidly until at approximately 2 ms and 7 mm, annotated by (1) in Fig. S1, it reaches a minimum as ignition effects decay and before full chemistry driving a self-sustaining flame has developed. Thereafter, S_n increases rapidly during the transition from spark assisted to self sustaining flame propagation [3]. After approximately 4 ms and 10 mm (point (2)), chemistry appears to be well established with S_n exhibiting a continuous increase with time and radius.

Shown in Figure S2 are Flame images for isooctane/air mixture at phi 1.4. Images for three separate tests are shown at different ignition energies and times to further illustrate the level of repeatability of the experiment.

Shown in Figs. S3 and S4 are variations of flame speed with: (a) time; (b) radius and (c) rate of stretch for methane /air mixtures and isooctane/air respectively at ϕ=1.1. Shown in figure S4 is data for isooctane and air mixtures at ϕ=1.2. In all cases, the pressure and temperature were the same as for Fig. S1 (and Figures 1-4 in the main paper) and data for ignition energies of 11, 16, 36 and 53 mJ are shown unless the mixture failed to reliably ignite. Each curve in Figs. S1 and S3 to S5 represent the average from 3 explosions and the error bars represent the typical extent of their variation..

Figures S6 to S9 show results for the same experimental conditions as figures 1 to 4 (i.e.methane/air mixtures and iso-octane/air mixtures at ϕ=0.8 and ϕ=1.4, T=358 K, P=0.3 MPa) but at a larger scale so that the early stages can be more clearly seen

Fig. S10 shows isooctane-air mixture (ϕ=1.1, T=358 K, P=0.3 MPa) at both extreme ends of the ignition energies tested: At both the extreme energies there appears to a be a linear region of evolution in the S_n variation against α. The low and high α limits of the data used for linear extrapolation are denoted by the symbols * and # respectively. This data range corresponds to flame growth from a radius of approximately 15 mm to 30 mm and was considered sufficient for extrapolation. It is clear that all the images of the flame at 11 mJ are distorted and wrinkled in comparison to those at the highest energy. The important point is that for the higher energy case, this linear region is close to that for a self-sustaining smooth spherical flame and hence Eq. (2) is appropriate. However, for the low energy case, the structure is wrinkled and, although it appears linear, the measured S_n and α are those for an evolving wrinkled and distorted flame with an increased surface area. Without an examination of flame structure and the variation of this structure at different energies, this could be easily misconstrued to be a valid data range for fitting of Eq. (2). This necessitates an examination of the flame images to be taken into simultaneous consideration while deciding upon the appropriateness of the data range to be used. The gradients of the linear regions imply measured L_b' values to be different, i.e. L_b'~0.33 mm and 0.53 mm at 11 and 53 mJ respectively. Here the L_b' obtained by linear fitting to the higher energy case, which is closer to being smooth and spherical, should be close to the true intrinsic value, while that for the low energy case is different with a relative error of 38% due to invalidity of applying Eq. (2).

Figures

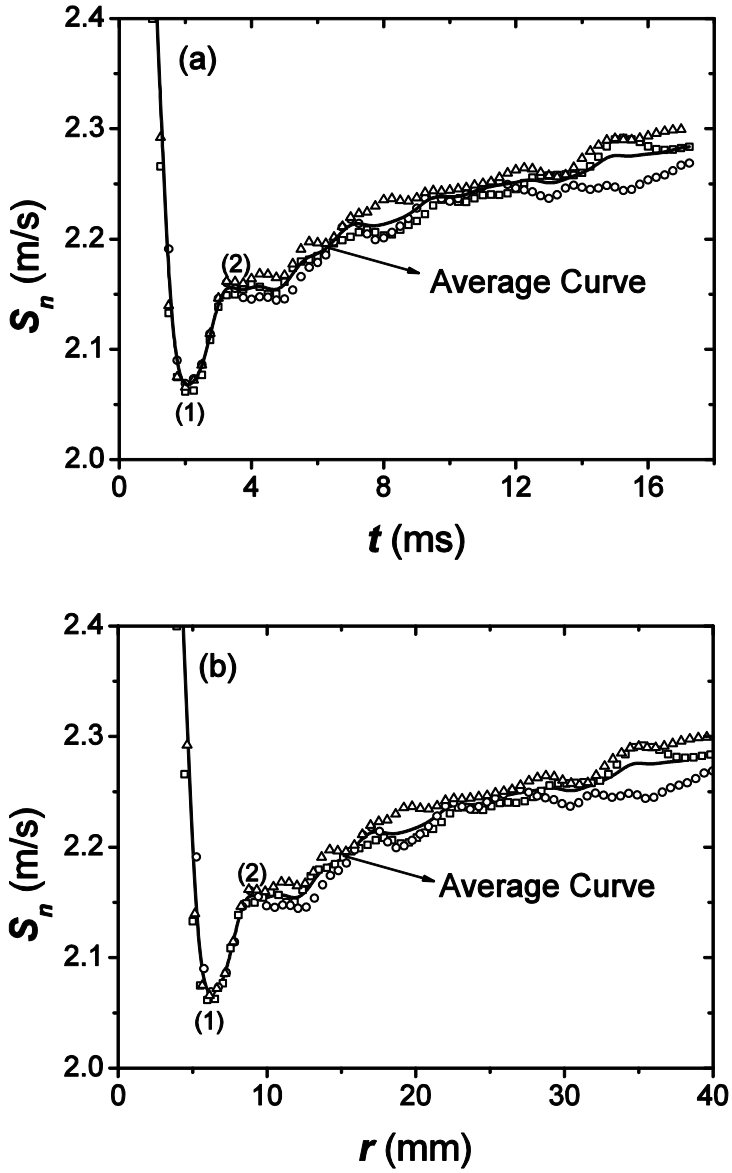

Figure S1 : Variation of S_n with (a) time and (b) radius. Methane-air mixture (ϕ =1.1, T=358 K, P=0.3 MPa). The symbols show results from three individual explosions at ignition energy of 36 mJ.

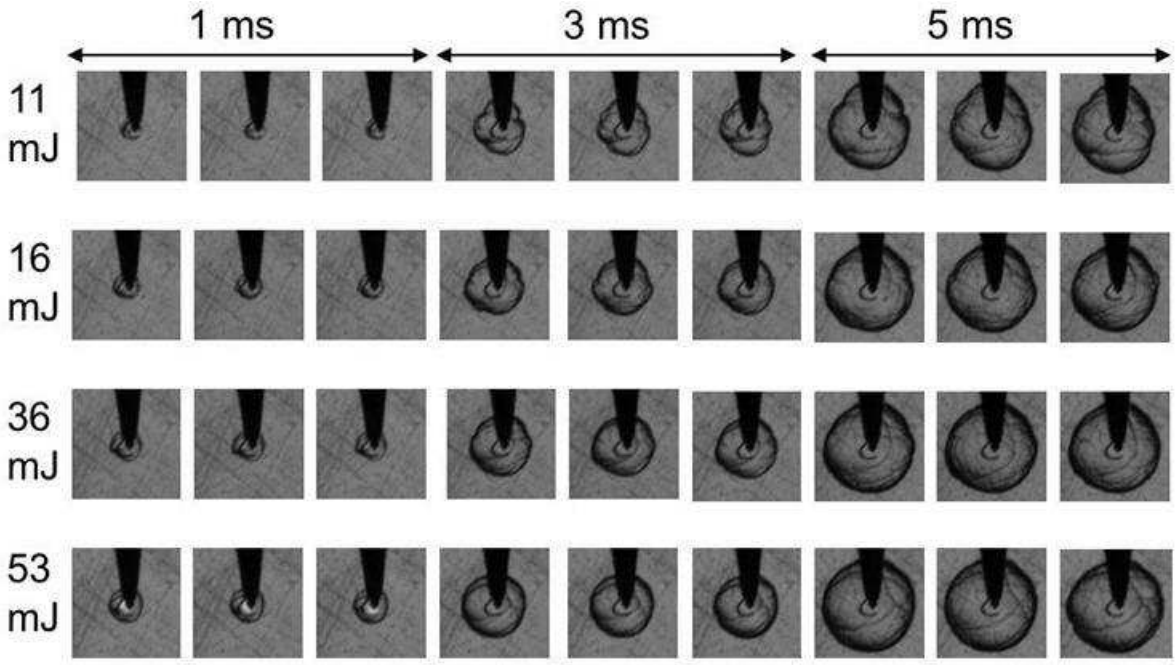

Figure S2 : Images of explosions of iso-octane–air mixtures (phi =1.4) for different ignition energies at 1ms, 3ms and 5ms to illustrate the repeatability of the technique

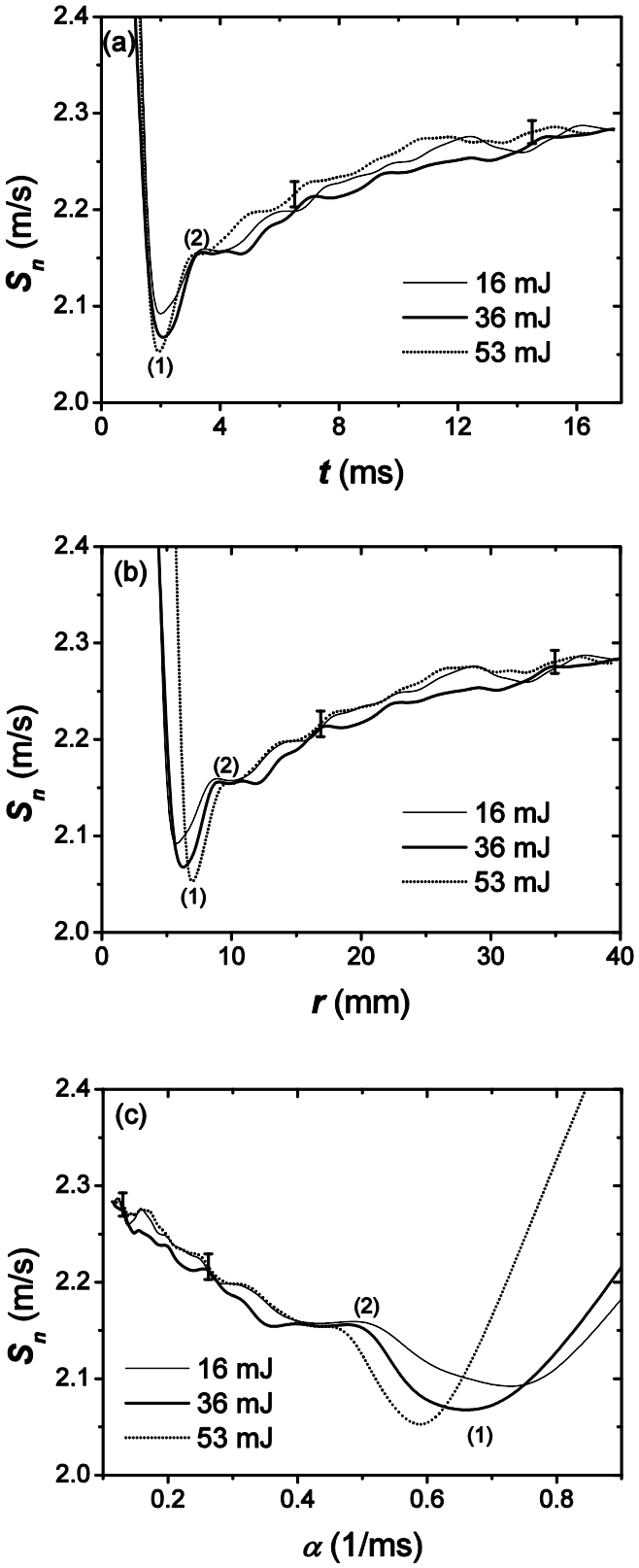

Figure S3 : Variation of S_n with (a) time; (b) radius and (c) stretch rate at different ignition energies. Methane-air mixture (ϕ =1.1, T=358 K, P=0.3 MPa).

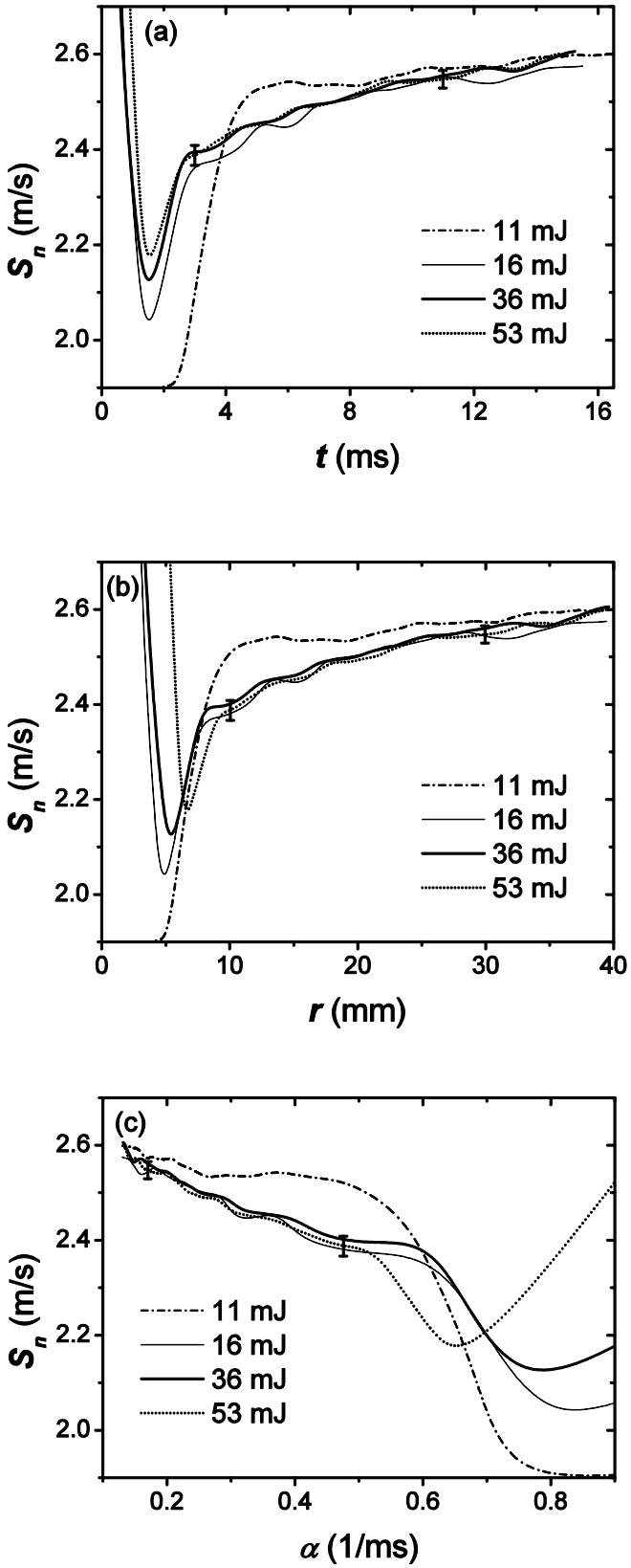

Figure S4 : Variation of S_n with (a) time; (b) radius and (c) stretch rate at different ignition energies. Isooctane-air mixture (ϕ =1.1, T=358 K, P=0.3 MPa).

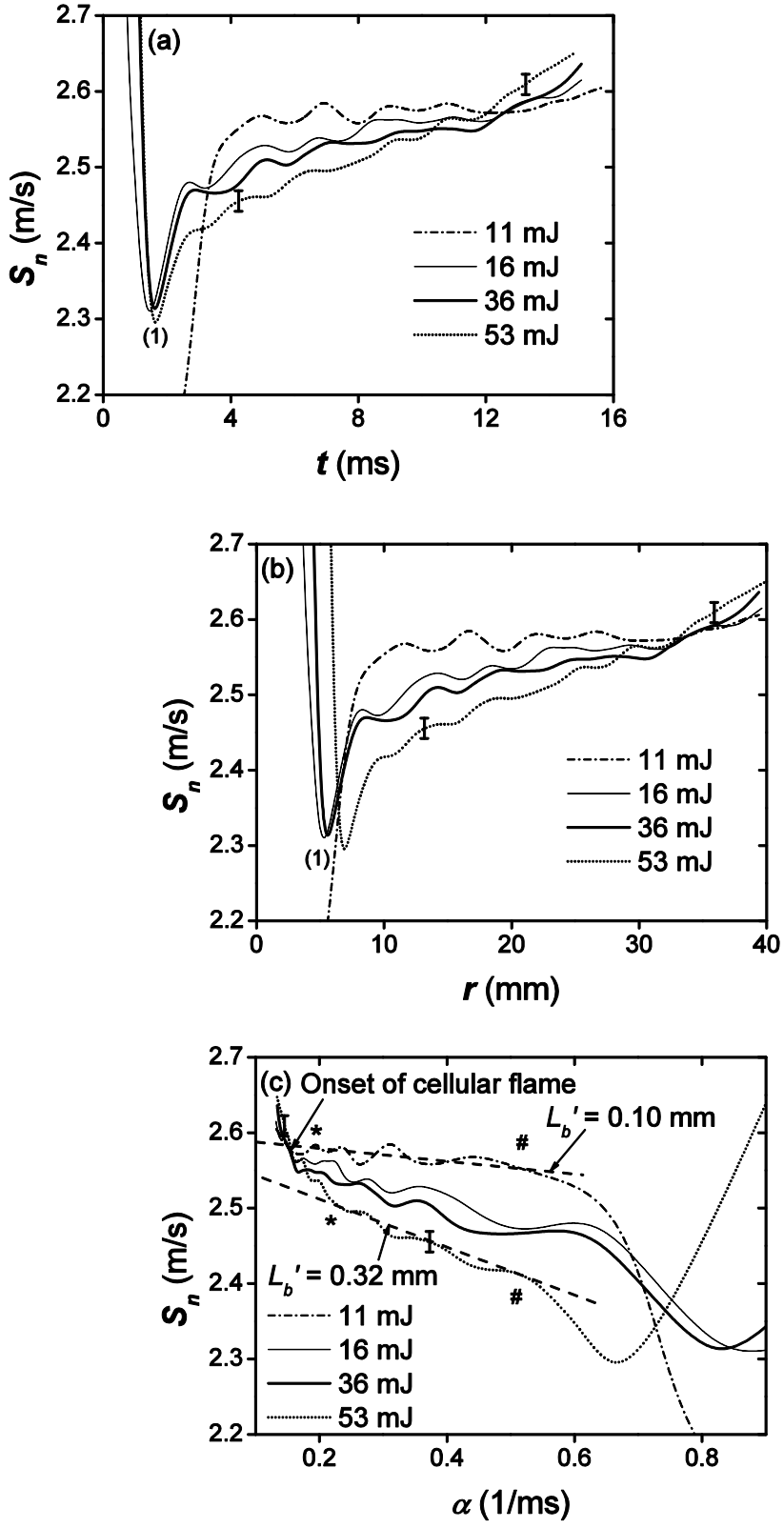

Figure S5 : Variation of S_n with (a) time; (b) radius and (c) stretch rate at different ignition energies. Isooctane-air mixture (ϕ=1.2, T=358 K, P=0.3 MPa). The symbols # and * denote the start and end of the linear range used to obtain L_b' as discussed in Section 3.2.

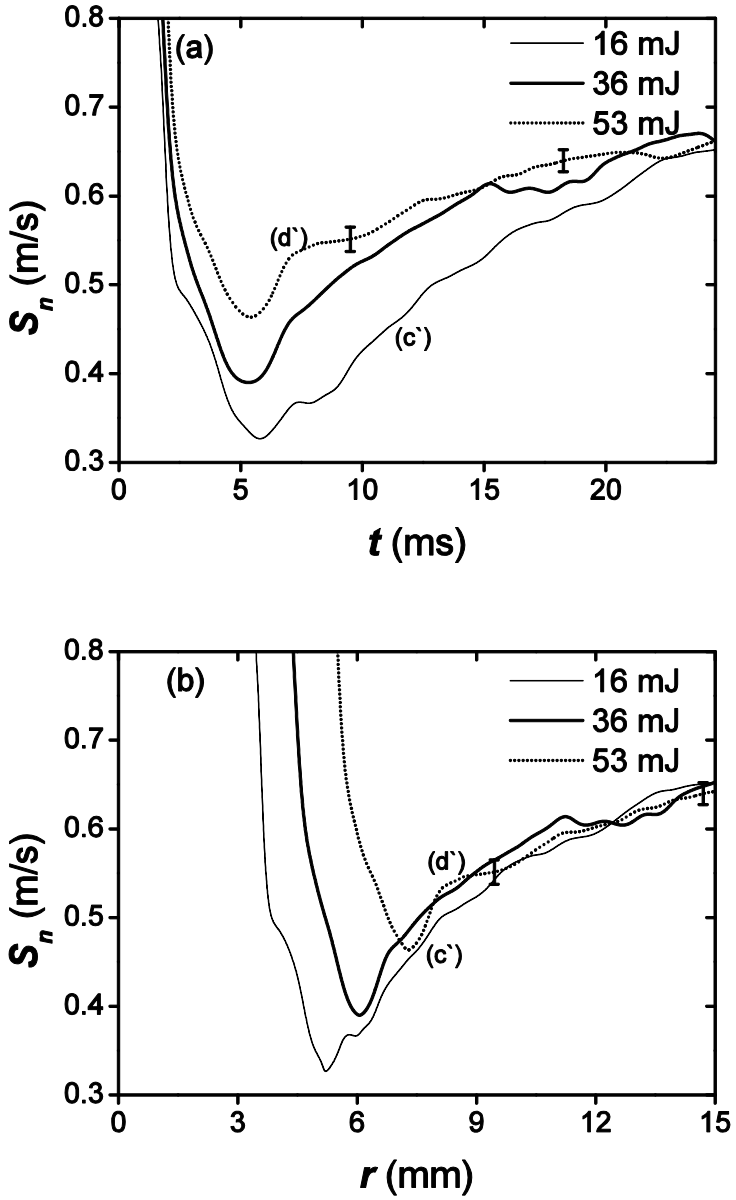

Figure S6: Variation of S_n with (a) time and (b) radius at different ignition energies. Methane-air mixture (ϕ=1.4, T=358 K, P=0.3 MPa). Points (c`) and (d`) refer to flame image (c) and (d) respectively in Fig. 6.

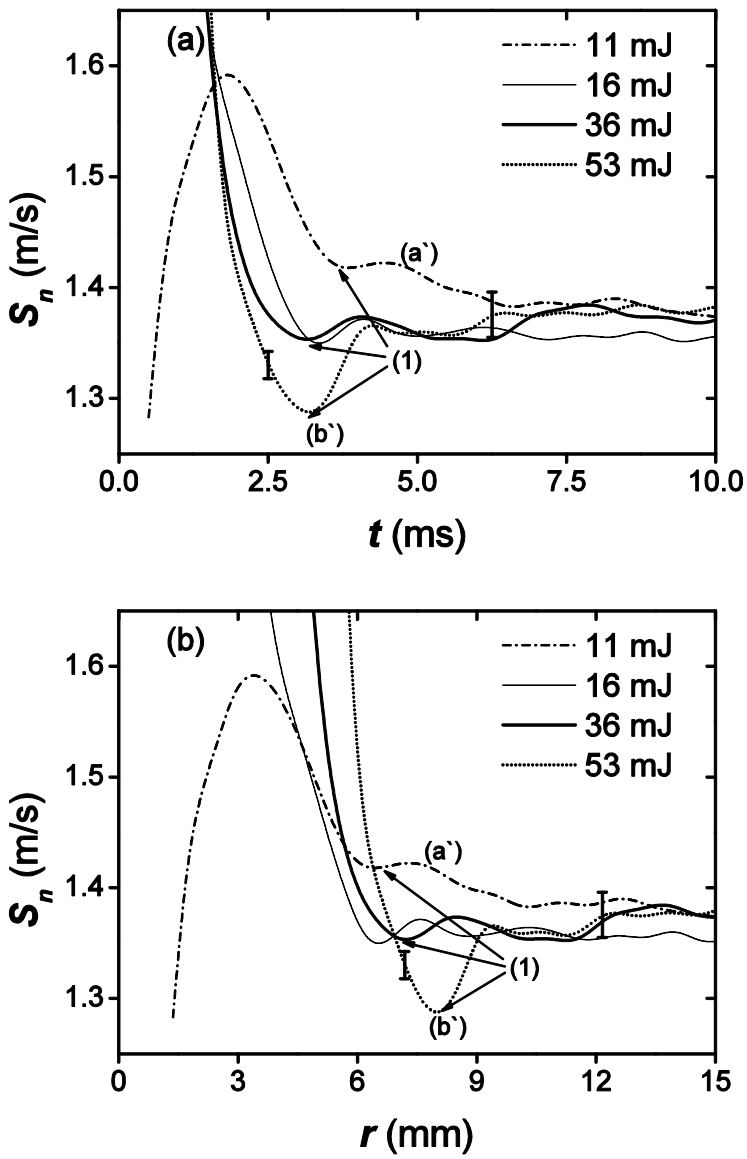

Figure S7: Variation of S_n with (a) time and (b) radius at different ignition energies. Methane-air mixture (ϕ=0.8, T=358 K, P=0.3 MPa). Points (a`) and (b`) refer to flame image (a) and (b) respectively in Fig. 6.

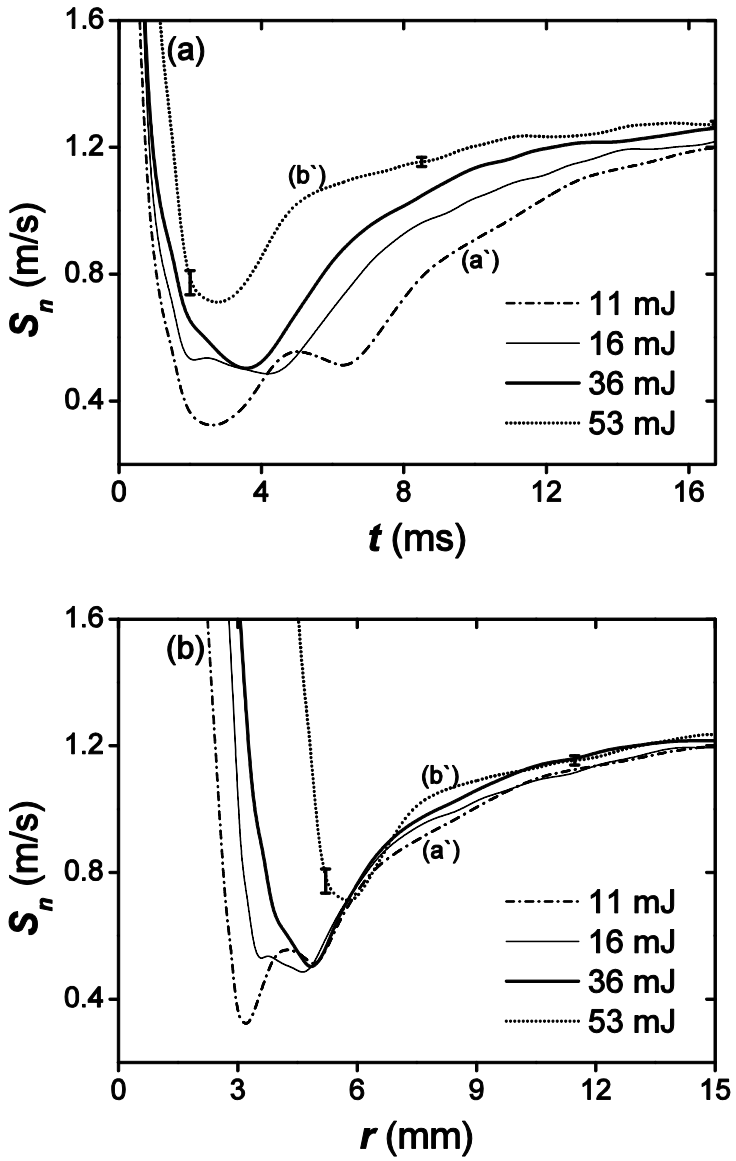

Figure S8 : Variation of S_n with (a) time and (b) radius at different ignition energies. Isooctane-air mixture (ϕ=0.8, T=358 K, P=0.3 MPa). Points (a`) and (b`) refer to flame image (a) and (b) respectively in Fig. 5.

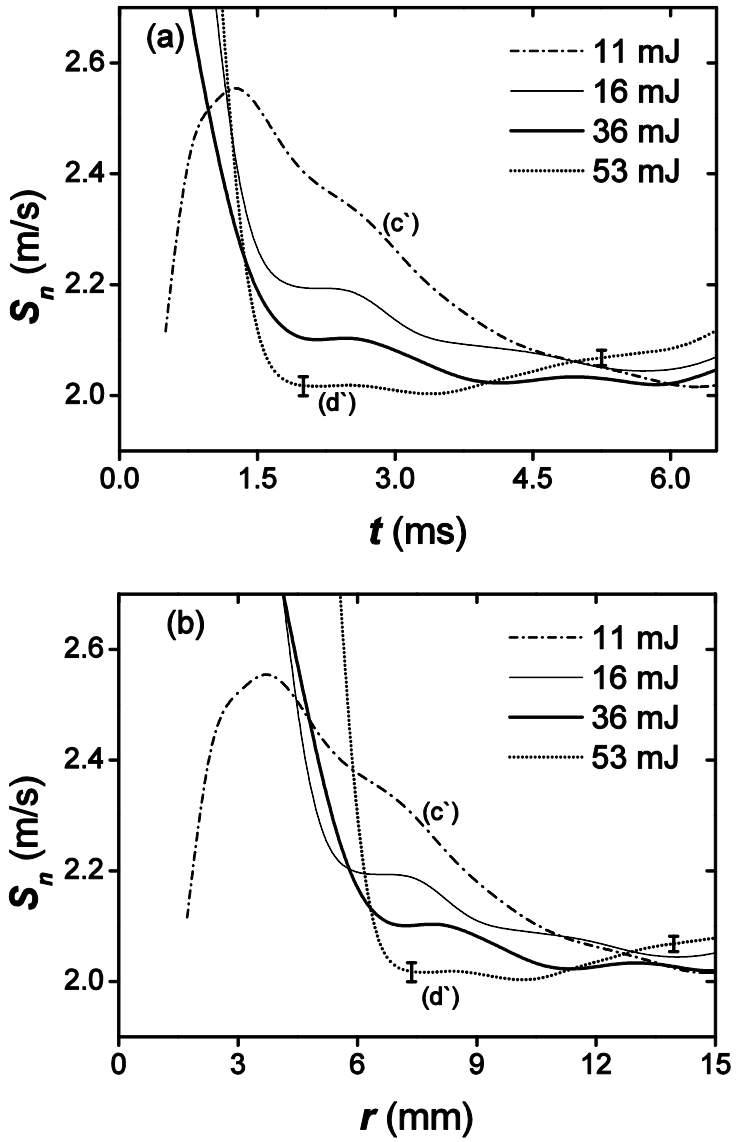

Figure S9 : Variation of S_n with (a) time and (b) radius at different ignition energies. Isooctane-air mixture (ϕ=1.4, T=358 K, P=0.3 MPa). Points (c`) and (d`) refer to flame image (c) and (d) respectively in Fig. 5.

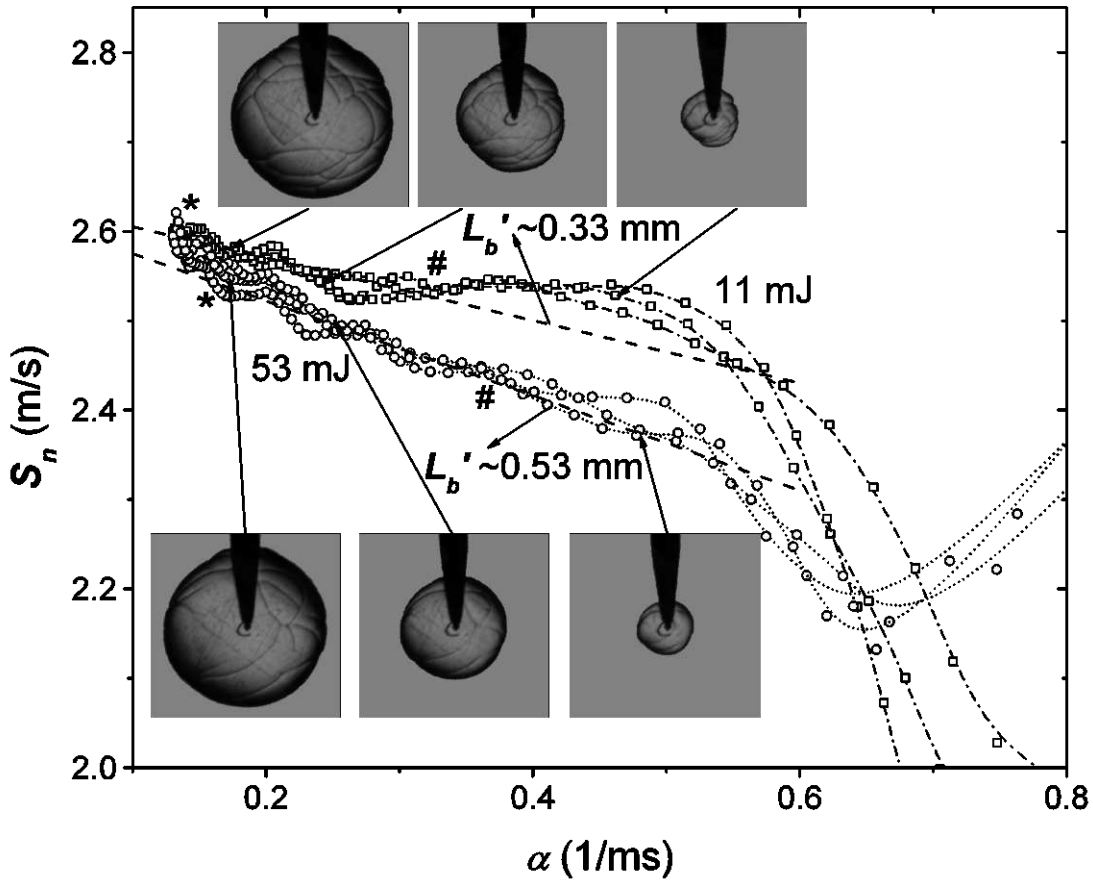

Figure S10 : Variation of S_n with α, three explosions each at ignition energy of 11 and 53 mJ. Isooctane-air mixture (ϕ=1.1, T=358 K, P=0.3 MPa). The symbols # and * denote the start and end of the linear range used to obtain L_b'.